

Long-Term Biocompatibility of a Miniature Stimulator Implanted in Feline Hind Limb Muscles

Tracy Cameron,* Member, IEEE, Tiina L. Liinamaa, Gerald E. Loeb, and Frances J. R. Richmond

Abstract— Chronic foreign-body responses and muscular changes were examined following the implantation of active miniature stimulators into the hind limb muscles of cats for periods of up to three months. The radio-frequency (RF)-powered stimulators were injected into muscles through a 12-gauge hypodermic needle. The tissue responses around the active stimulators were compared histologically to those provoked by passive devices, broken glass, silicone tubing, polyester suture material coated with polybutylate, and two of the internal components of the stimulator (ferrite, integrated circuit chip). Active and passive stimulators produced similar, benign foreign-body reactions that resulted in an essentially identical fibrous capsule over time. The responses were similar to those produced by the internal components and the suture material, and were more modest than those produced by the broken glass. The capsule did not appear to interfere with the functionality of active devices because thresholds measured during the post-implantation survival period did not change significantly over time. Unexpectedly, the severity of the reaction differed significantly amongst the various target muscles. Medial gastrocnemius exhibited the most severe response, whereas tibialis anterior had the least reaction.

Index Terms— Electrical stimulation, FES, FNS, paralysis, TES.

I. INTRODUCTION

IN clinical practice, devices that apply electrical stimulation to muscles most commonly use electrodes placed on the skin to deliver the stimulus pulses. However, advances in microtechnology now make it possible to construct implantable stimulators that can be inserted directly into muscles or next to nerves. One such miniature device consists of a cylindrical glass package with an electrode sealed hermetically into each end [1], [2]. It receives power and data from a single amplitude-modulated radio-frequency (RF) field via inductive coupling. This new technology eliminates many of the problems encountered with surface stimulation. However, all implanted medical devices are foreign bodies that trigger tissue changes whose effect on device performance and the health of the recipient must be understood before they can be used clinically.

One method used to assess the biocompatibility of an implanted device is to evaluate the tissue response using light

Manuscript received December 20, 1996; revised February 24, 1998. This work was supported by the Ontario Rehabilitation Technology Consortium, the Canadian Neuroscience Network of Centres of Excellence, and the National Institutes of Health (NIH) under Contracts N01-NS-2-2322 and N01-NS-5-2325. Asterisk indicates corresponding author.

*T. Cameron is with Advanced Neuromodulation Systems, Inc., 1 Allen-town Parkway, Allen, Texas 75002 USA (e-mail: tracy@ans-medical.com).

T. L. Liinamaa, G. E. Loeb, and F. J. R. Richmond are with Queen's University, Kingston, Ont. K7L 3N6 Canada.

Publisher Item Identifier S 0018-9294(98)05325-7.

microscopy. Tissue implanted with a foreign body undergoes a series of inflammatory reactions that occur, in part, as a response to the surgical process itself. During the first 24 to 48 h following implantation, tissue can show redness (due to local vascular dilation), heat (due to increased local blood flow), swelling (due to increased local vascular permeability), and pain (due to local accumulation of chemical mediators) [3]. The severity of the inflammatory response is thought to be in part related to the nature of the protein layer formed on the surface of the implant [4], [5]. The type of protein that most readily is absorbed onto the surface of an implant will depend on the materials composing the implant [6], [7]. For example, proteins such as albumin do not contribute to the inflammatory response [8], whereas fibrinogen can elicit the accumulation of large numbers of phagocytic cells [9].

The acute inflammatory response usually resolves after about a week. Over subsequent months, the implant becomes encapsulated by a progressively more fibrous layer of connective tissue [3]. If the device is highly biocompatible, the capsule is generally quite thin, and the interface between it and the device contains only a few macrophages. When devices provoke continued tissue reaction, the surrounding connective tissues are thicker, more vascularized, and disorganized, and they contain large numbers of necrotic cells and leukocytes. The continued presence of leukocytes indicates possible infection and/or biological degradation of the implant itself.

The surface materials of the new implantable stimulator tested in this study [1] are borosilicate glass, and tantalum and iridium metal. Individually these materials have been found to be highly biocompatible [10]–[14]. In a recent study, Fitzpatrick *et al.* [15] showed further that a stable, fibrous capsule formed around similarly shaped but passive glass devices and stimulators that were implanted in muscle for a period of two months.

In this study, we examined the long-term performance as well as the tissue response of active and passive miniature stimulators. First, we used histological methods to compare the tissue responses around the active stimulators to those provoked by passive devices, broken glass, silicone tubing, polyester suture material coated with polybutylate, and two of the internal components of the stimulator [ferrite, integrated circuit (IC) chip]. This was done by implanting the materials into hind limb muscles of cats for periods of up to three months. Second, we examined the long-term performance of the stimulator by measuring thresholds of stimulation for muscle, weekly, over this period. Our results showed that active and passive miniature stimulators elicit similar, benign foreign body reactions that progress to form essentially identical

TABLE I
SCORING KEY USED IN THE ANALYSIS OF TISSUE IMPLANTED WITH ACTIVE AND PASSIVE DEVICES, COMPONENTS, AND OTHER MATERIALS

	Weight factor	1	2	3	4
PMN's	3	1-20	21-40	41-60	61+
Lymphocytes	2	1-20	21-40	41-60	61+
Macrophages	1	1-10	11-20	21-30	31+
Giant cells	2	1	2	3	4
Fibroblasts	1	1-10	11-20	21-30	31+
Capsule thickness	NA	0-15 mm	.15-.3 mm	.3-.45 mm	.45+ mm
Muscle fiber characteristics (<100 μm)	2	minimum	mild	moderate	severe
Muscle fiber characteristics (<100 μm)	3	minimum	mild	moderate	severe
Fibrosis	NA	minimum	mild	moderate	severe

Cell counts were made within a 0.01 mm² area under 1000× magnification.

TABLE II
LIST OF THE ANIMAL NUMBER, LOCATION OF IMPLANT, DURATION OF IMPLANT, DURATION OF STIMULATION AND INITIAL THRESHOLD VALUES FOR EACH CAT IMPLANTED WITH ACTIVE DEVICES

Implant location (cat ; muscle)	Device ID #	Implant duration/ stimulation days	Initial threshold	
			Current (mA)	Pulse width (ms)
Max : R soleus	052/85	101/65	0.4	100
Max : R nerve medial gastrocnemius	053/1	101/37	1.0	100
Max : R tibialis anterior	037/4	101/65	0.6	100
Max : R extensor digitorum longus	054/5	101/65	0.8	100
Percy : R soleus	055/85	105/69	0.4	60
Percy : R nerve medial gastrocnemius	058/6	105/69	0.4	50
Percy : R tibialis anterior	059/63	105/69	1.2	120
Percy : R extensor digitorum longus	057/255	105/69	0.8	110
Biawy : R posterior biceps femoris	060/6	56/30	0.6	120
Biawy : R semitendinosus	062/31	56/30	0.4	130
Biawy : R anterior sartorius	061/32	56/30	1.2	60
Biawy : R medial sartorius	056/85	56/30	1.6	130

fibrous capsules over time. This reaction did not appear to interfere with the functionality of the device because thresholds measured during chronic implantation did not change significantly over time. We did find, however, that the severity of the reaction appeared to differ amongst the various host muscles.

II. MATERIALS AND METHODS

A. Surgical Preparation

Experiments were carried out on nine cats (2.8–4.2 kg; either sex) anesthetized with sodium pentobarbital (initial dose, 35 mg/kg ip; supplemental doses, 5 mg/kg iv). Cats were placed in one of two groups to test the biocompatibility of A, devices ($n = 4$) or B, components ($n = 5$). In each cat of group A, four devices were implanted using aseptic techniques in right hind-limb muscles and activated for up to three months and four nonactivated (passive) devices were placed in the comparable left hind-limb muscles (Table I). In each cat of group B, muscles in each hind-limb were implanted with passive devices, silicone tubing (Silastic, Dow Corning, Midland, MI), broken glass tubing of the kind used in the external capsule (Kimbrel borosilicate glass type N51A; Friedrich & Dimmock, Millville, NJ), or one of two internal components (integrated circuit chips or ferrite pieces) (Table II). To insert the tested devices or components two skin

incisions were made in each limb. One incision extended along the anterior surface of the shank, and the other along the posterior surface from the popliteal fossa to the calcaneum. In all but one animal in group A, devices or components were inserted parallel to the muscle fibers in each of the following muscles: tibialis anterior (TA), extensor digitorum longus (EDL), medial gastrocnemius (MG), and either soleus or lateral gastrocnemius (LG). In one cat of group A, one active and passive device was implanted into the right and left semitendinosus, biceps femoris, and anterior and medial sartorius muscles. This latter procedure was performed to assess any differences in tissue reactions between muscles with in-series versus pinnate fiber architectures. In all cases intact devices were injected using a 12-gauge angiograph insertion tool (Becton Dickinson Vascular Access; Sandy, UT). Components were introduced by making a small channel in the muscle tissue by blunt dissection with fine scissors and inserting the device with fine forceps. A single suture (6-0 Ethibond, Ethicon Ltd., Peterborough, Canada) was tied at the muscle-entry site to prevent the device from migrating out of the muscle, and to aid in locating the device at the time of removal.

B. Stimulation

Animals were trained to recline in a tube (8-in diameter × 18-in long) for 2 h/day by using palatable food as an

incentive. The transmitting coil that sent data and power to the implant was wrapped around the outside of the tube. After surgery the animals recovered for three to five days. Stimulation settings (pulse width and current amplitudes) required to produce threshold twitches of the muscle were determined for each active device. Current twice or four times threshold was used during daily stimulation, applied while alert animals fed or rested in the tube (Table I). Each device was activated at 4-s intervals using trains of stimuli at 20 Hz for 1 s. Stimulators were activated in pairs (one flexor and one extensor) producing co-contractions, thus reducing the movement of the limb. Stimulus trains were applied for two hours a day, five days a week, for a period of up to three months.

C. Weekly Measurements

Once a week, threshold measurements were made for all implanted active devices (Fig. 2). Animals were anaesthetized using intramuscular injection of ketamine hydrochloride (Rogarsetic, Rogar/STB Inc.; 9 mg/kg) and xylazine (Rompun, Haver; 0.5 mg/kg) to eliminate voluntary muscle contractions. Thresholds were obtained by setting the current amplitude to the lowest setting still able to produce a palpable muscle twitch using the maximal pulse width of 258 μ s. The pulse width was decreased in 1- μ s steps, until the twitch was no longer detected.

D. Terminal Measurements

For the terminal procedure, two cats from group A were anaesthetized by intravenous injection of sodium pentobarbital (as above). TA and EDL muscles were removed from the distal insertion and attached to a strain gauge (Fig. 1). Isometric twitch and train forces were measured using a force transducer (measured linear up to 35 N; compliance 8.9 μ m/N) attached to the tendon of insertion. The force transducer was attached to a motor-driven puller that was used to adjust whole-muscle length. A bone screw was fastened to the tibia and fibula and secured to the frame of the puller to fix the origins of the muscles. Contractions were elicited by stimulating muscle nerves either with the implanted stimulator or from the sciatic nerve using a nerve cuff. This allowed comparison of the maximal force output of each muscle produced by an active device with that produced using a nerve cuff.

At the end of each test period all implants were removed from the animals and examined under a dissecting microscope and environmental scanning electron microscope (ESEM; model E-3, Electroscan) for any visible damage or changes in surface characteristics. These results are discussed in a previous report [2].

E. Tissue Processing

Each muscle was weighed and cut into small transverse blocks (2 cm \times 2 cm \times 2 cm). The blocks were mounted on aluminum disks using embedding medium (OCT compound, Ames) and the anatomical orientation of each block was recorded. Muscle blocks were coated with talcum powder and immersed into liquid nitrogen (-196°C) for storage.

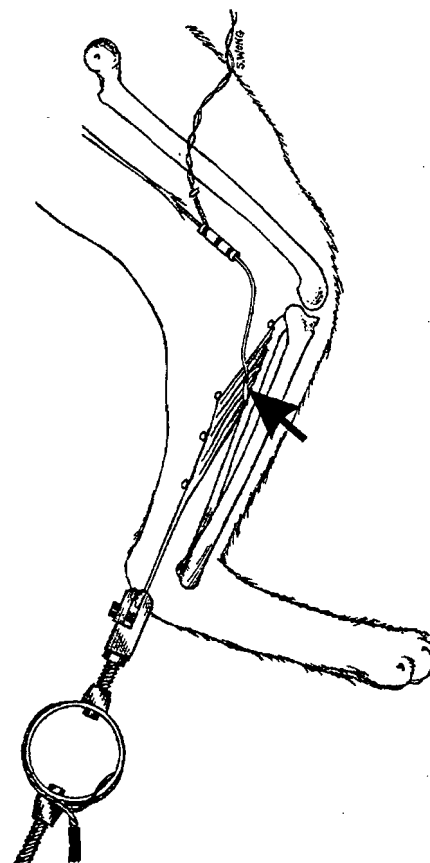


Fig. 1. Line drawing of the terminal experimental preparation showing the location of the microstimulator (arrow) with respect to muscle landmarks. The distal end of the muscle is attached to a force transducer. A nerve cuff was placed around the muscle nerve proximal to its insertion into the muscle.

The blocks were warmed to -20°C and cut into 15–18 μm transverse sections. Two or more adjacent cryostat sections were retained at 2-mm intervals. Sections were placed on gelatin coated slides and dried in a 60°C oven for 30 min. The tissue was stained with either haematoxylin and eosin (H&E) or picrosirius red [16]. At least one additional section was taken from each block and stained for adenosine triphosphatase (ATPase) activity after formalin fixation and alkaline (pH 10.4) preincubation [17]. Stained muscle sections were examined under a light microscope.

F. Data Analysis

The cellular reaction and the overall tissue response to the implants and the suture material (6-0 Ethibond, Ethicon) marking the site of muscle entry were examined using a light microscope. Within the reactive zone counts were made of polymorphonuclear leukocytes (PMN's), lymphocytes and plasma cells, macrophages, fibroblasts, and giant cells. Cells were counted in five randomly selected 0.01 mm^2 regions within the capsule on each slide under $1000\times$ magnification by two investigators, one of whom was double-blinded. Results of the observations were reviewed with a neuropathologist (J. Rossiter, Queen's University, Kingston, Ont., Canada). The cell counts were given a score ranging from zero to four (adapted from American Society for Testing and Materials

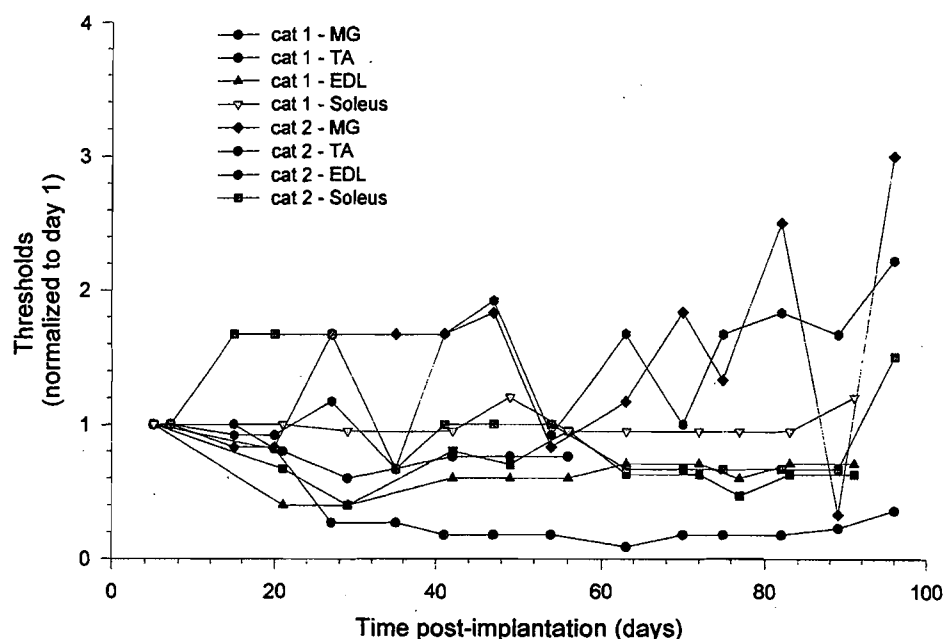


Fig. 2. Threshold settings (normalized to day one) as a function of time (days post-implantation). Thresholds were measured weekly for the duration of the experiment.

TABLE III
LIST OF THE ANIMAL NUMBER, LOCATION OF IMPLANT, AND
DURATION OF IMPLANT FOR EACH CAT IMPLANTED WITH
PASSIVE DEVICES, MATERIALS, AND STIMULATOR COMPONENTS

Implant location (cat : muscle)	Material	Implant duration (days)
N144 : R medial gastrocnemius	glass	30
N144 : R lateral gastrocnemius	silicone tubing	30
N144 : L medial gastrocnemius	ferrite	30
N144 : L lateral gastrocnemius	IC chip	30
N165 : R medial gastrocnemius	intact stimulator	30
N165 : R lateral gastrocnemius	silicone tubing	30
N165 : L medial gastrocnemius	glass	30
N165 : L lateral gastrocnemius	ferrite	30
N166 : R medial gastrocnemius	intact stimulator	30
N166 : R lateral gastrocnemius	silicone tubing	30
N166 : L medial gastrocnemius	glass	30
N166 : L lateral gastrocnemius	ferrite	30
N167 : R medial gastrocnemius	intact stimulator	30
N167 : R lateral gastrocnemius	silicone tubing	30
N167 : L medial gastrocnemius	glass	30
N167 : L lateral gastrocnemius	ferrite	30
N168 : R medial gastrocnemius	intact stimulator	30
N168 : R lateral gastrocnemius	silicone tubing	30
N168 : L medial gastrocnemius	glass	30
N168 : L lateral gastrocnemius	ferrite	30
Romeo : R (belly) lateral gastrocnemius	passive device	33
Romeo : L (belly) lateral gastrocnemius	passive device	33
Romeo : L (distal) biceps femoris	passive device	33
Romeo : R (distal) biceps femoris	passive device	33
Romeo : Tibialis anterior	passive device	33
Romeo : R (belly) medial gastrocnemius	passive device	33
Romeo : R (nerve) medial gastrocnemius	passive device	33

individual cell score by a weight factor. Weight factors were assigned in a manner that reflected the significance of a particular cell type in the inflammatory response, and adapted from the ASTM standards (Vol. 13.01).

The implant site was further evaluated for fibrosis and abnormal muscle fiber characteristics (Fig. 3). A quantitative score from zero to four was assigned, with zero being not present and four being a severe reaction. The fibrosis score was determined by examining the thickness of the endomysium and perimysium in the tissue surrounding the implant. A score of one (minimum) was assigned when less than 50 muscle fibers in the perimeter of the capsule were surrounded by thickened connective tissue (greater than 10- μm thick). A score of two (mild) was assigned when 50 to 100 muscle fibers were surrounded by thickened connective tissue. A score of three (moderate) was assigned when greater than 100 muscle fibers were surrounded by thickened connective tissue. Finally, a score of four (severe) was assigned when most of the muscle fibers around the perimeter of the implant (>75%) were surrounded by thickened connective tissue. Muscle fiber characteristics, such as size, ATPase staining, and location of myonuclei, were examined in two sites, one less than 100 μm and the other greater than 100 μm from the implant. Abnormal muscle fibers were identified by their rounded shape, small (< 50- μm) diameter, and/or centrally located nuclei. A score of one (minimum) was assigned when only a small localized region of abnormal fibers (<50 cells) was observed and there still existed a distinct boundary between muscle fibers and capsule. A score of two (mild) was assigned when a larger number of nonlocalized muscle fibers (50–100 cells) appeared abnormal, and when some of these fibers (<20 cells) were separated from other fibers by connective tissue. A score of three (moderate) was assigned when more than 50% of the perimeter of the implant was surrounded

(ASTM) standards, Vol. 13.01; see Table III), recorded on a score sheet, and the scores from the five sites were averaged. An overall cell score was calculated by multiplying each

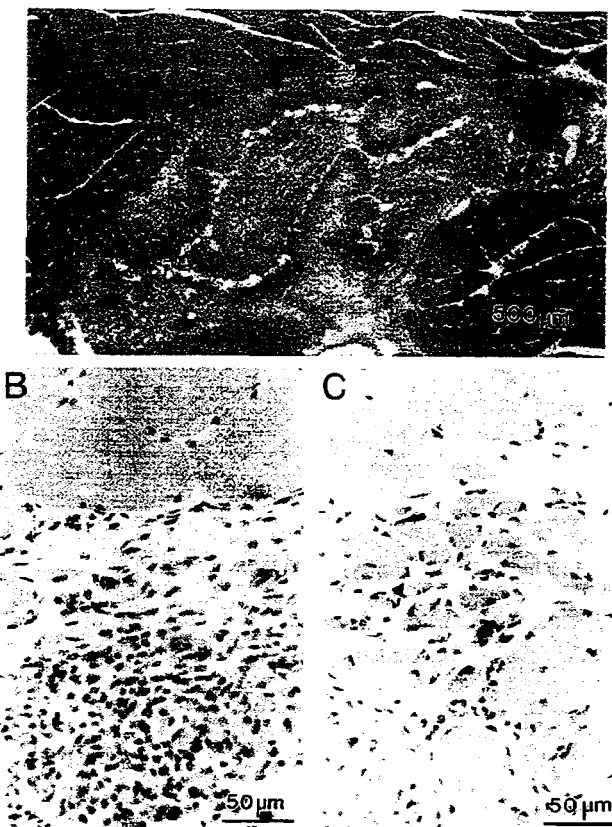


Fig. 3. Photomicrographs of an implantation site in the medial gastrocnemius muscle that contained an active device. Tissue sections were stained with hematoxylin and eosin. (A) Typical features of the capsule and cellular response visualized at low magnification; (B) a high magnification of the fibrous capsule and cellular response; (C) a region of abnormally small muscle fibers at the edge of the capsule with centrally located nuclei.

by abnormal muscle fibers, many of which (<50 cells) were surrounded by a thick ($<10 \mu\text{m}$), cellular connective tissue and inflammatory cells appeared to invade some of the muscle fascicles. Finally, a score of four (severe) was assigned when greater than 75% of the perimeter was surrounded by abnormal muscle fibers, separated by large amounts of connective tissue ($>10 \mu\text{m}$), and when muscle fibers and inflammatory cells were loosely mixed. A single score to reflect muscle-fiber characteristics was calculated by multiplying the two scores from different sites by a weight factor. A factor of two was used for sites less than $100 \mu\text{m}$ from the capsule, and a factor of three was used for sites greater than $100 \mu\text{m}$ from the capsule. A large weight was given for damage seen further away from the capsule, because changes would indicate a more severe response. Finally, a measurement was made of the capsule thickness by first drawing the implant site under $250\times$ or $400\times$ magnification using a camera lucida attachment on a microscope, and then digitizing the traces using the frame-grabbing software, BioScan Optima (version 2). The capsule thickness measurement included a thin fibrous layer surrounding a thicker cellular region. An average of five measurements was recorded for each section through an implant site. When the capsule was situated on the perimeter of the muscle, part of the capsule was often torn or folded blurring the extent of the capsule and prohibiting

thickness measurements. These regions were not analyzed quantitatively.

We tested for any differences between the severity of the reaction, assessed by quantitative scores, and the type of implant or type of host muscle by performing two-sample *t*-tests, and one-way analysis of variance (ANOVA) using statistical functions in Microsoft Excel. We grouped the muscles according to whether they had active or passive device implants and tested for any changes in the various scores over time by performing linear regression on data from cats euthanized at different survival times. The results were plotted using a Sigma Plot graphing package.

III. RESULTS

A. Observations of Device Performance: *In Situ*

All devices that were activated by RF coupling caused muscle contractions that could be readily palpated through the skin. The contractions were well tolerated by the cats, who showed little interest in their moving limb and commonly slept during the stimulation session. In a single instance in which an active device was placed into the right semitendinosus, the cat began to lick a circumscribed region of skin over the posterior surface of the right hind-limb about four weeks post-implantation. The cat showed no other signs of sensitivity or gait disturbance. Nevertheless, the fact that the cat focussed unusual attention on this site prompted us to interrupt the experiment at five weeks to look for a source of irritation that might explain this behavior. Histological examination of the implanted muscle revealed a circumscribed but unusual pattern of damage in the right semitendinosus muscle, described below.

Of the 12 active devices that were implanted, only one stopped working before the end of the experiment (for summary see Tables I and II, device 053). This failure was due to a leak in the glass seal that allowed body fluids to enter the device and short circuit the electronics. During the course of each experiment, device functionality was assessed during the sessions at which weekly thresholds were measured for each implanted device. Fig. 2 shows those measurements normalized to the values on day one for eight devices implanted into the hind-limb muscles of two cats for approximately three months. No relationship was found between the threshold measurements and the number of days that the devices were implanted, as determined by calculating the correlation coefficient for the data corresponding to each device.

Twitch forces measured during the terminal experiments for two cats implanted with active devices were calculated to be approximately 10% of maximum. In one cat stimulated chronically at $2\times$ threshold, the twitch force was 13.8% of maximum in the EDL muscle and 6.5% in the TA muscle. In another cat, stimulated at $4\times$ threshold, twitch forces of 10% were recorded in soleus, and forces of 26% were recorded in TA.

B. Tissue Responses

1) *Active and Passive Devices:* All implanted devices triggered a benign inflammatory response similar to that described previously for miniature stimulators and glass capsules with

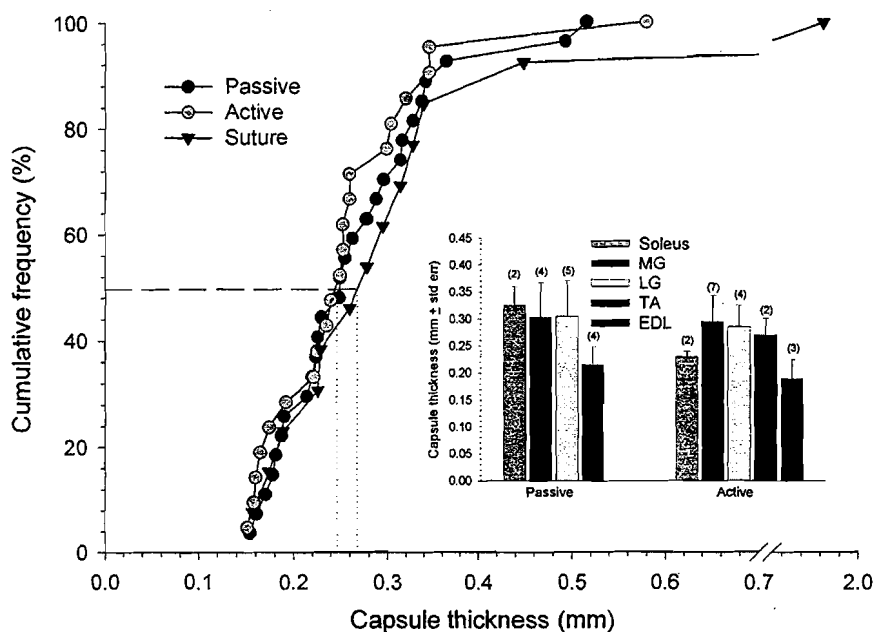


Fig. 4. Cumulative frequency as a function of capsule thickness (mm) for active devices, passive devices, and suture material. The dotted line shows the median size of capsule. Insert shows the capsule thickness (score) as a function of muscle type for active and passive devices.

similar dimensions [15]. Devices removed after 30, 56, and 100 days were surrounded by a well-defined outer capsule that contained an accumulation of macrophages and leukocytes (Fig. 3). Inspection of sections cut at different levels along the length of the device, from the tantalum to the iridium end, did not show any consistent differences in capsule thickness or cellular accumulations.

Analysis of foreign-body reactions focused upon two types of changes: changes that occurred in normally present tissues, including muscle fibers and connective tissues; and features of new tissues provoked by the inflammatory reaction. Examinations of muscle and connective tissues suggested that devices had modest effects that did not differ significantly for active or passive devices. ATPase staining of fibers revealed the presence of three distinct fiber types whose relative proportions were similar when fascicles abutting the fibrous capsule were compared to fascicles further from the implant site. In addition, muscle fibers immediately adjacent to the capsule surrounding a device were usually normal in size and pattern of nucleation (Fig. 3). Less than 10% of fibers abutting the fibrous capsule had cross-sectional diameters less than 50 μm or had centrally placed nuclei, as shown in Fig. 3(b) and (c). When atrophic fibers were seen, they were often confined to a single fascicle in which all fibers were shrunken. The enzyme profiles of these shrunken fibers were similar to those of nearby large fibers, and the fascicle displayed a similar mosaic of fiber types.

Although changes in muscle fibers were infrequent in all muscles, significant differences were found in the scores assigned to muscle-fiber characteristics when the various muscles chosen for implant were compared. Implant sites around devices from medial gastrocnemius had greater numbers of abnormal muscle fibers located throughout the perimeter of the capsule. Fibrosis close to the implant site was also a characteristic feature that was similar in its appearance when sites around active and passive devices were compared. Fibrosis

was generally observed to be less than 10- μm thick throughout the site, but the fibrosis score assigned to implant sites taken from soleus and medial gastrocnemius were found to be statistically higher than from lateral gastrocnemius and tibialis anterior. This was reflected in a more extensive distribution of perimysial thickening between muscle fiber fascicles in MG and soleus compared to TA.

The foreign-body reaction that surrounded the implanted devices had two main constituents, an outer, encapsulating layer of fibrous, cell-poor material, and an internal accumulation of loosely packed inflammatory cells. The fibrous capsules, which included both layers, did not differ significantly in thickness between muscles implanted with active or passive devices, or between different host muscles. Interestingly, the capsules were also similar in thickness to capsules around the suture material at the site of implant (Fig. 4). Half of the capsules surrounding the active and passive devices were under 0.24 mm, whereas half of those around suture material were under 0.27 mm. The fibrous layer component was found to be only 20% of the overall capsule thickness measurement. Thus, half of the fibrous capsule layers surrounding the active and passive devices were under 0.05-mm thickness.

Accumulations of inflammatory cells within the fibrous capsule were composed predominately of macrophages. Lymphocytes were present more rarely. They were found in occasional clumps at implant sites in which the overall reaction was judged to be most severe. The type of host muscle appeared to affect significantly the severity of the response as reflected in the significant differences between cell scores amongst the various host muscles. In order to eliminate this difference when comparing the responses of implanted active and passive devices, an additional analysis of active versus passive devices was confined to the 20 sampled sections from two active and two passive devices implanted in MG, the muscle demonstrating the most severe reaction. No significant

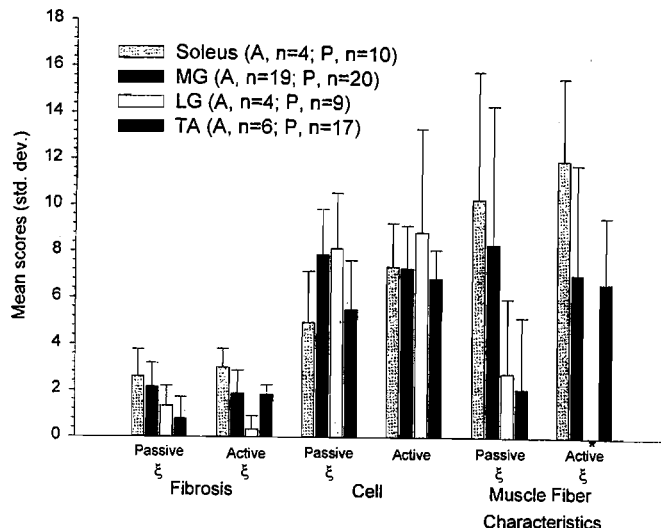
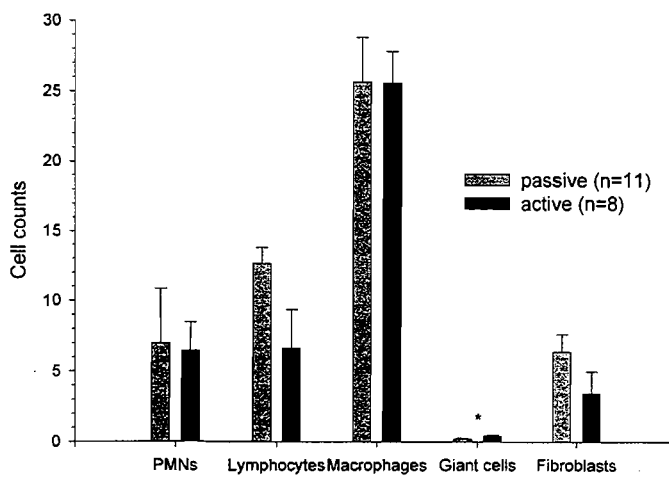


Fig. 5. Fibrosis score, cell score, and muscle-fiber score for active and passive devices as a function of muscle type; ξ indicates a significant difference between muscles ($p < .05$). Fibrosis score was out of a maximum of four. Cell score was calculated by summing the five weighted individual cell scores giving a maximum score of 36. Muscle-fiber score was calculated by summing the weighted muscle score $<100 \mu\text{m}$ with the weighted muscle score $>100 \mu\text{m}$ giving a maximum score of 20. (See Table I for details.) *Note, the average muscle score for LG was zero.

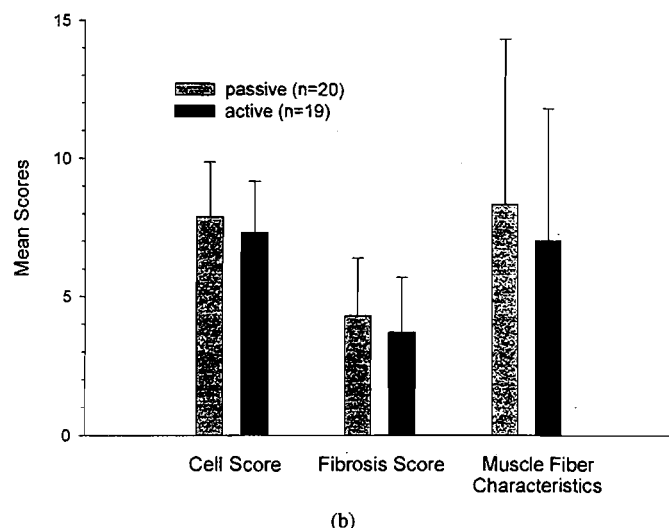
differences were found between overall cell scores, fibrosis scores and muscle-fiber scores sampled from the sites around active and passive devices (Fig. 5). However, a significant difference ($p < 0.05$) was found between the numbers of giant cells associated with active and passive devices [Fig. 6(a)]. These results must be interpreted with caution because the number of giant cells in each sample was very small and subject to potential sampling bias (active devices <0.4 cells, passive devices <0.1 cells, in a typical 0.01-mm^2 field). No significant differences were found for any other cell types. A typical inspected region contained less than 20 PMN's, ten lymphocytes, 35 macrophages, and ten fibroblasts. The number and type of cells did not change significantly in muscles implanted for 30–100 days.

Devices implanted into semitendinosus, biceps femoris, and anterior and medial sartorius of a single cat produced similar fibrous capsule formation as described above. However, upon examining the semitendinosus muscle under the patch of skin that the animal had been licking, we found an unusual region of damage that began at the level of the tantalum electrode (effective cathode) and extended into the interfascicular connective tissue toward the tendinous inscription that separates the two neuromuscular compartments of this muscle (Fig. 8). The muscle fibers in this region appeared smaller in diameter than elsewhere in the muscle. The perimysium surrounding each fiber was thicker and more cellular than that surrounding fibers in undamaged regions of the same section.

2) Internal Components and Controls: When comparisons of capsule formation were extended to other implanted materials, the thickness of the fibrous capsule was found to vary with the type of implant (Fig. 7). A thin connective tissue sheath containing a variety of inflammatory cells surrounded components. The number of cells varied according to the type



(a)



(b)

Fig. 6. (a) Cell score, fibrosis score, and muscle-fiber score for active and passive devices in the medial gastrocnemius muscle. Fibrosis score was out of a maximum of four. Cell score was calculated by summing the five weighted individual cell scores giving a maximum score of 36. Muscle-fiber score was calculated by summing the weighted muscle score $<100 \mu\text{m}$ with the weighted muscle score $>100 \mu\text{m}$ giving a maximum score of 20. (See Table 4.2 for details). (b) Cell counts for active and passive device implants for the medial gastrocnemius muscle. (average of five sites) *indicates a significant difference ($p < .05$) between active and passive implants.

of implanted material. Glass shards and silicone tubing were implanted to act as positive and negative controls, respectively. Thus, the most severe reactions and the thickest capsules were found when broken glass was implanted. In some sections we observed up to 100 PMN's in a 0.01-mm^2 area near the centre of the reactive site. However, the glass shards were contained within a capsule and showed no signs of migrating out of the site of implantation. Components (ferrite pieces and IC chip) did not cause any observable differences in foreign-body response and the overall appearance of the capsules was identical to that described above for active and passive devices. The least severe reaction and thinnest fibrous capsule occurred around the soft silicone tubing. The capsule thickness was measured to be only 0.05 mm and contained little, if any, cellular reaction. All capsules appeared to be stable except those produced by the glass shards, which showed a continuing

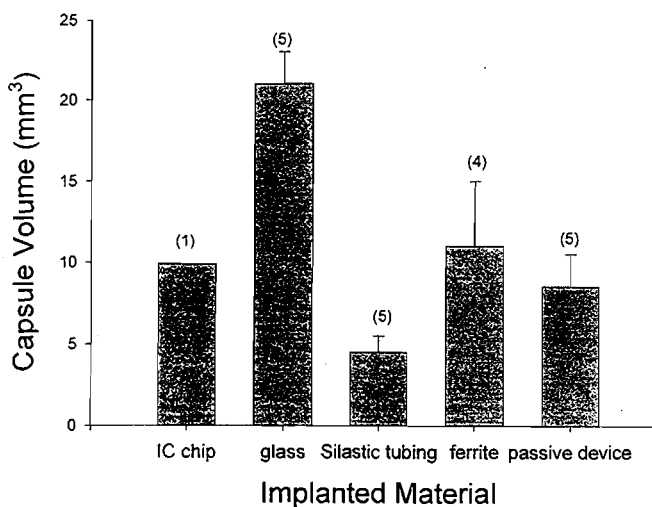


Fig. 7. Capsule volume as a function of the implanted material. The capsule volume is largest for the broken glass pieces and smallest for the Silastic tubing. (n) indicates the number of samples in each group.

presence of leukocytes and debris typical of a nonresolving inflammatory reaction.

IV. DISCUSSION AND CONCLUSIONS

In the present study, we examined the foreign-body response to passive and active miniature stimulators and compared this response to that elicited by suture material, silicone tubing, broken glass capillary tubes, or internal components that comprise the stimulator. We found that active and passive devices elicited a similar reaction. Two lines of evidence led us to conclude that this reaction was stable over time. First, weekly threshold measurements for eliciting muscle contractions did not change significantly over time for any of the active devices. Second, histological assessments of host tissue revealed the presence of a stable foreign-body response similar to that produced by any nontoxic biomaterial [18]. We also found that the host muscle used for implantation appeared to affect the amount of damage caused by the implant. This observation is important for two reasons. First, it suggests that our results cannot be compared directly with studies in which implants are placed in paraspinal or gluteal muscles, often in other species. Second, it suggests that the specific reaction of a muscle to a relatively benign implant can depend as importantly on muscle-specific characteristics as device-specific characteristics.

A. Methodological Considerations

The methodologies adopted in this study were chosen to facilitate the simultaneous study of several aspects of the muscle response. These modifications in experimental design must be kept in mind when comparing the results reported here with descriptions of histopathology reported typically in the literature. Most studies that assess biocompatibility use thin, paraffin-embedded sections [3]. However, in this study, frozen sections were used so that muscle fibers could be examined using histochemical methods to identify changes in enzyme profiles. These frozen sections were up to three times thicker

than sections cut typically from paraffin blocks. Consequently, counts of inflammatory cells made on regions of similar size should be about three times higher than those anticipated by previous cell-scoring methods based on paraffin sections [3]. To compensate for the difference in section thickness, we adjusted our scoring methods for all cellular counts.

In addition, it was necessary to retrieve the devices prior to histological analysis. Retrieval was made difficult because the irregular shape of the device had encouraged connective tissues to envelop and anchor the device firmly, especially at its tantalum end. The elaboration of connective tissues at the tantalum end of the device is consistent with observations of connective-tissue ingrowth in other studies of chronically implanted, porous or roughened materials [18], [19]. The need to cut the connective tissues anchoring the device and drag the device through the encapsulating space probably caused local tissue disruption and redistribution of the cellular material within the capsule around the device. This disruption was felt to account, at least in part, for the relatively large standard deviation in some quantitative measures from different sampled sites.

One problem that was encountered during evaluation of histopathological changes was the relative generality of published criteria to score foreign-body responses. For example, it is a generally accepted practice to score fibrotic or muscular changes according to whether they are minimum, mild, moderate, and severe. These criteria assume a level of understanding of histopathology that may not exist amongst researchers who do not conduct such evaluations routinely. Further, it poses the potential for confusion when two different observers have slightly different interpretations about scoring criteria. Thus, we have attempted to specify in more detail the scoring methods that we developed for the present study. The scores for fibrosis were found to be the most troublesome because the degree of perimysial thickening around the device was generally modest, and variations in perimysial thickness were common even in different parts of seemingly unaffected muscle far from the implanted site. Thus, scores for fibrosis should be interpreted cautiously.

B. Foreign Body Response Elicited by Implanted Stimulators

Previous studies have suggested that the introduction of a nonabsorbable foreign body initially involves the death of cells and tissues. This reaction resolves over time, as a fibrous connective tissue coat encapsulates the material. All of our tissue was examined one month or more following implantation, well after the time when we would expect to observe cell death. Thus, we were not surprised by the failure to see necrotic changes. Persistent necrosis changes should occur only in response to the release of local toxic substances, which are unlikely to come from the highly inert metals and glass comprising the casing of the stimulators. The cellular response that we did observe was consistent with that which occurs during the healing process. The most common cells were macrophages and lymphocytes, which have important roles in the repair process, and are commonly found at the site of an inflammatory response [20], [21]. In addition, we found the occasional giant cell. Giant cells are formed at

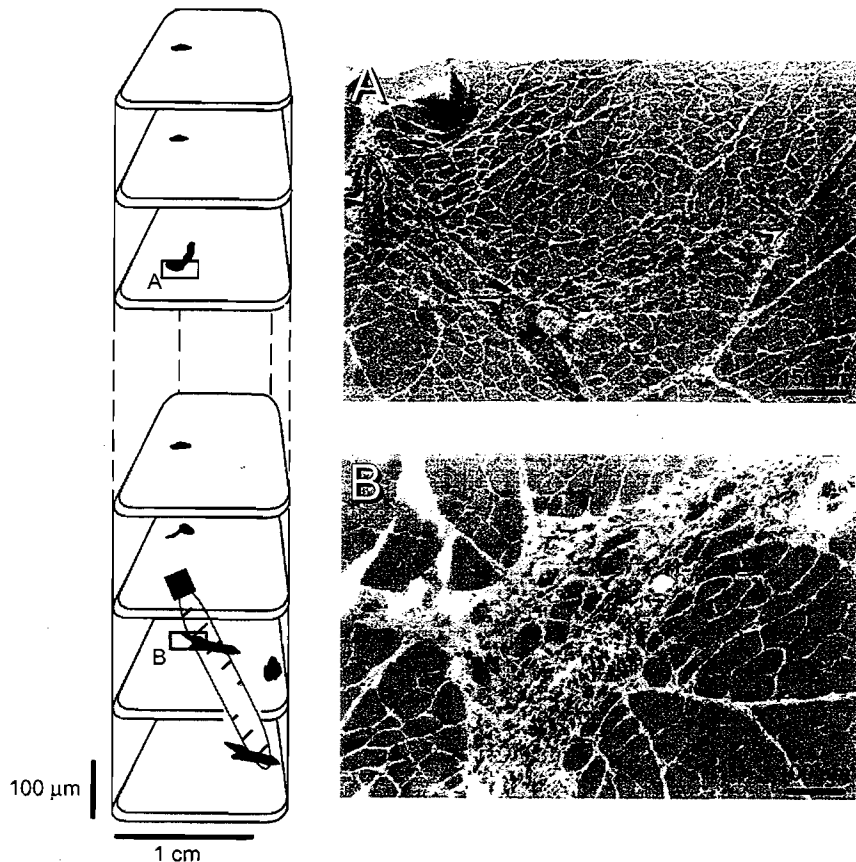


Fig. 8. Diagram of the damaged region in the semitendinosus muscle with respect to the location of the stimulator. Insert (A) is a photomicrograph of the damaged site in the semitendinosus muscle proximal to the device; (B) photomicrograph of the implantation site in the semitendinosus muscle stained with hematoxylin and eosin in the region around the active device.

sites of chronic inflammation from the fusion of monocytes, newly arriving from the blood, with aging macrophages [22]. They are found most commonly when implants have multiple filaments (e.g. sutures) or irregular surfaces. We had suspected that we might see more giant cells at the tantalum end of the electrode, because the tantalum electrode is rougher than other parts of the stimulator, but this did not prove to be the case. However, any conclusions about giant-cell distribution must be guarded because tissue disruption during the removal of the stimulator may have obscured any changes in cellular accumulations at the tantalum end of the electrode.

Acute inflammation typically results in the accumulation of PMN's. These cells are released at the site of inflammation and disappear four to six days after the cause for the inflammation has been removed [3]. Because very few of the sites implanted with microstimulators were found to contain PMN's, we concluded that the reactions were relatively stable. However, PMN's were present consistently in muscle implanted with broken glass pieces, suggesting a persistent rather than resolving inflammatory response. The continuing inflammation most likely was due to continued tissue damage caused by the movement of the sharp material within the muscle.

C. Stability of Electrical Thresholds

The above cellular responses suggest that a stable reaction occurred at the site of the active and passive stimulators. This

conclusion was supported further by threshold measurements, which were not found to change significantly over time. In fact, many of the thresholds decreased when compared to threshold values measured on the first day after surgery. This improvement in threshold was thought to result from a reduction in swelling and inflammation and removal of any necrotic tissue produced by the initial insertion procedure.

There are two reasons why stimulus thresholds were considered to be a useful gauge of reaction stability. First, a gradual increase in threshold might have been prognostic for a progressive increase in capsule thickness that might displace the stimulator away from excitable elements over time. Second, a change in threshold might have suggested device migration. The relative stability in stimulus threshold that was in fact observed was consistent with the histopathology showing little change in the 300- μm separation created by the foreign-body response between the device and the adjacent excitable tissue. Nevertheless, the foreign-body response appeared to be an effective barrier to device migration, as has been identified elsewhere for devices of similar size [15]. Device migration was also, presumably, hampered by the extensive ingrowth of connective tissues around the tantalum electrode. Guyton and Hambrecht [19] reported previously that material accumulated in the pores of a tantalum electrode much like that used here. The ingrowth of tissue was found to increase the pore resistance of the electrode to 2–3 times that measured

immediately after implantation. However, Guyton and Hambrecht [19] found no significant changes in the threshold of motor responses during a six-month period of testing. Both these and present results suggest that immobilization of the stimulator by the foreign-body reaction effectively prevents device migration, which would be detected by a change in threshold as the device moved closer or further from bundles of motor axons in the muscle (for further discussion see [15]). Whether this adhesion to the surrounding tissue is beneficial or detrimental to the evolution of the foreign-body response remains to be determined.

Changes in muscle fibers close to the encapsulation were generally modest. Rarely did a muscle fascicle contain fibers smaller than average in size. However, when such atrophy did occur it was often found in all of the fibers composing one or more fascicles. The changes might be attributed to the damage or section of one or more small nerve branches at the time of implantation. The stable enzyme profiles of fibers adjacent to the device suggested that damage did not occur selectively in any one fiber type and that the stimulation was relatively innocuous. Further, no differences were found between active and passive devices under the conditions of the study. It remains possible that active devices could produce more damage or changes in enzyme levels if they were used to stimulate the muscle for longer periods of time. Damage to muscles by prolonged stimulation can follow the improper or overenthusiastic use of any stimulator and can be produced even by vigorous natural exercise [24]. The regime adopted for the work described here is typical of protocols used elsewhere for clinical rehabilitation of spinal cord injured patients [25], [26].

In a single instance, we observed muscle-fiber damage that was unusual and might have been caused by muscle stimulation. This damage occurred in a semitendinosus muscle, a muscle known to be composed of in-series fibers [27]. We might speculate that the in-series architecture of the semitendinosus contributed to the development of this modest region of damage. In some series-fibered muscles, it is possible to stimulate more muscle fibers at one muscle end than the other [28], [29], by submaximal motor unit activation. Such asymmetrical activity has been shown to cause nonuniform length changes along the length of the muscle, so that muscle fibers at the weaker end must work under lengthening (eccentric) conditions. A range of physiological studies have shown that muscle damage is relatively common after vigorous eccentric contractions [30], [31]. Thus, stimulation of muscles in a pattern that might cause eccentric conditions in some muscle parts may set up shear forces that have a damaging effect, even if the device itself is biocompatible.

Most of the implanted materials or components that were studied produced a similar inflammatory response regardless of the size, shape, or composition. Only the broken glass pieces caused damage to cross-sectional areas of muscle greater than 1 mm^2 and this response was the only one that did not appear to resolve. Silicone tubing was found to produce the least amount of damage and to result in a capsule whose thickness was less than one-fifth that of the reaction zone measured around the glass shards. The modest reaction to silicone tubing is consistent with previous studies

that generally attribute its biocompatible nature to its benign chemical constituents. However, silicone tubing was also the softest material implanted and might have the least tendency to abrade moving muscle fibers during the vigorous contractions that hind-limb muscles can be expected to generate under free-ranging behavioral conditions.

D. Does the Muscular Target Matter?

The thickness of the capsule around implanted stimulators did not vary significantly amongst the different muscles. However, several other features of the foreign-body response differed depending upon the type of muscle that was implanted. Tibialis anterior consistently showed the least severe response whereas soleus and medial gastrocnemius tended to exhibit greater responses. The reasons for such differences cannot be determined from this type of study. Nevertheless, we might speculate that the severity of muscle reaction might be related to the architecture and activity level of the muscle into which the device is implanted. The usage patterns of cat hind-limb muscles are known to differ substantially even though their fiber-type compositions are often similar. For example, Ariano [32] has shown that MG and TA both have approximately 60% fast-glycolytic and 20% slow-oxidative fibers. However, MG is an extensor and is active during standing and the entire stance phase, whereas TA is a flexor and active mostly while shortening is unopposed during the swing phase of walking [33]. During normal walking the stance phase has been found to last twice as long as the swing phase. The more continual contractions and higher forces in MG might lead to a greater mechanical abrasement of muscle tissue around the rigid implanted device. Alternatively, the varying degree of damage that is seen in different host muscles may relate to some intrinsic, but as yet poorly understood feature of muscle structure and performance. For example, Lexell *et al.* [34] has raised the possibility that stimulation-induced damage can vary in a manner related to muscle architecture. He electrically stimulated rabbit TA and EDL muscles at several different frequencies under essentially identical conditions and found that damage in EDL was consistently greater than in TA, for all frequencies.

The finding that muscles show differences in their foreign-body reactions is an important observation for protocols that aim to evaluate the biocompatibility of devices for regulatory or other purposes. Most, if not all, biocompatibility testing is performed in conformance to standards developed using the paravertebral muscles of rabbits or the gluteal muscles of rats (ASTM Standards, Vol. 13.01). Paraspinal muscles of sedentary or restrained animals may rarely be active and, thus, may not move repeatedly against the hard surfaces of an implanted device. In such a situation we might expect the most benign of muscle reactions. However, more damage might be expected if the same implanted device were to be inserted into a different, highly active muscle. By implanting devices into the distal limb muscles of free-ranging cats, we feel the devices were subjected to a particularly severe biocompatibility challenge compared to responses reported by conventional testing. In the clinical environment, muscle stimulators such as those

examined here will be implanted in muscles with a high degree of variation in their architectures, usage patterns, age, and health. All of these variable factors add a significant level of complexity when designing and testing a generic system that will be used for several applications.

ACKNOWLEDGMENT

The authors would like to thank Dr. J. Rossiter for assistance in the analysis of the pathology, J. Creasy for assistance with the surgery and preparation of the figures, and J. Conway for assistance in the statistical analysis.

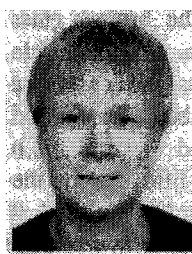
REFERENCES

- [1] G. E. Loeb, C. J. Zamin, J. H. Schulman, and P. R. Troyk, "Injectable microstimulator for functional electrical stimulation," *Med. Biol. Eng., Comput.*, vol. 29, pp. 13-19, 1991.
- [2] T. Cameron, G. E. Loeb, R. A. Peck, J. H. Schulman, P. Strojnik, and P. R. Troyk, "Micromodular implants to provide electrical stimulation of paralyzed muscles and limbs," *IEEE Trans. Biomed. Eng.*, vol. 44, pp. 781-790, Sept. 1997.
- [3] S. C. Woodward and T. N. Salthouse, "The tissue response to implants and its evaluation by light microscopy," in *Handbook of Biomaterials Evaluation*, A. F. Von Recum, Ed. New York: Macmillan, 1986, pp. 364-377.
- [4] R. E. Baier and R. C. Dutton, "Initial events in interactions of blood with a foreign surface," *J. Biomed. Mater. Res.*, vol. 3, pp. 191-206, 1969.
- [5] V. I. Sevastianov, "Role of protein adsorption in blood biocompatibility of polymers," *CRC Crit. Rev. Biocompat.*, vol. 4, pp. 109-154, 1988.
- [6] J. D. Andrade and V. L. Hlady, "Plasma protein adsorption: The big twelve," *Ann. N.Y. Acad. Sci.*, vol. 516, pp. 158-172, 1987.
- [7] D. F. Williams, "Standard tests for soft tissue evaluation," in *Biomaterials and Clinical Applications*, A. Pizzoferrato, P. G. Marchetti, A. Ravaglioli, and A. J. C. Lee, Eds. Amsterdam, the Netherlands: Elsevier Science, 1987, pp. 783-790.
- [8] K. Kottke-Marchant, J. M. Anderson, Y. Umemura, and R. E. Marchant, "Effect of albumin coating on the *in vitro* blood compatibility of Dacron arterial prostheses," *Biomat.*, vol. 10, pp. 147-155, 1989.
- [9] L. Tang and J. W. Eaton, "Fibrin(ogen) mediates acute inflammatory responses to biomaterials," *J. Exp. Med.*, vol. 178, pp. 2147-2156, 1993.
- [10] B. Weiss, R. Stickler, S. Schider, and H. Schmidt, "Corrosion fatigue testing of implant materials (Nb, Ta, stainless steel) at ultrasonic frequencies," in *Proc. 1st Int. Conf. on Fatigue and Corrosion Fatigue up to Ultrasonic Frequencies*, Metallurgical Soc. AIME, Warrendale, PA, 1982, pp. 387-411.
- [11] H. Zitter and H. Plenk, Jr., "The electrochemical behavior of metallic implant materials as an indicator of their biocompatibility," *J. Biomed. Mater. Res.*, vol. 21, pp. 881-896, July 1987.
- [12] S. M. Slack and T. A. Horbett, "The effects of temperature and buffer on fibrinogen adsorption from plasma to glass," *J. Biomater. Sci., Polymer*, Ed., vol. 2, pp. 227-237, 1991.
- [13] J. S. Walter, J. McLane, W. Cai, T. Khan, and S. Cogan, "Evaluation of a thin-film peripheral nerve-cuff electrode," *J. Spinal Cord Med.*, vol. 18, pp. 28-32, 1994.
- [14] L. S. Robblee, J. L. Lefko, and S. B. Brummer, "Activated Ir: An electrode suitable for reversible charge injection in saline solution," *J. Electrochem. Soc.*, vol. 130, pp. 731-733, 1983.
- [15] T. L. Fitzpatrick, T. L. Liinaamaa, I. E. Brown, T. Cameron, and F. J. R. Richmond, "A novel method to identify migration of small implantable devices," *J. Long-Term Effects of Med. Implants*, vol. 6, pp. 157-168, 1996.
- [16] T. W. Weatherford, "Staining of collagenous and noncollagenous structures with picrosirius red F3BA," *Alabama J. Med. Sci.*, vol. 9, pp. 383-388, Oct. 1972.
- [17] L. Guth and F. J. Samaha, "Qualitative differences between actomyosin ATPase of slow and fast mammalian muscle," *Exp. Neurol.*, vol. 25, pp. 138-152, 1969.
- [18] T. N. Salthouse and B. F. Matlaga, "Some cellular effects related to implant shape and surface," in *Biomaterials in Reconstructive Surgery*, L. R. Rubin, Ed. St. Louis, MO: Mosby, 1983, pp. 40-45.
- [19] D. L. Guyton and F. T. Hambrecht, "Theory and design of capacitor electrodes for chronic stimulation," *Med., Biol. Eng.*, vol. 12, pp. 613-620, 1974.
- [20] I. Carr, *The Macrophages*. New York: Academic, 1972, pp. 1-60.
- [21] S. L. Robins and R. S. Cotran, *Pathologic Basis of Disease*, 2nd ed. Philadelphia, PA: Saunders, 1979, pp. 94-95.
- [22] T. J. Chambers, "Multinucleate giant cells," *J. Pathol.*, vol. 126, pp. 125-148, 1978.
- [23] D. L. Guyton and F. T. Hambrecht, "Capacitor electrode stimulates nerve or muscle without oxidation-reduction reaction," *Science*, vol. 181, pp. 74-76, 1973.
- [24] S. Salmons, "Exercise, stimulation and type transformation of skeletal muscle," *Int. J. Sports Med.*, vol. 15, pp. 136-141, 1994.
- [25] A. Kralj and T. Bajd, *Functional Electrical Stimulation, Standing and Walking After Spinal Cord Injury*. CRC: Boca Raton, FL, 1989.
- [26] R. B. Stein, T. Gordon, J. Jefferson, A. Sharpenberger, J. F. Yang, J. Totosy de Zepetnek, and M. Belanger, "Optimal stimulation of paralyzed muscle after human spinal cord injury," *J. Neurophysiol.*, vol. 72, pp. 1393-1400, 1992.
- [27] E. Smits, P. K. Rose, T. Gordon, and F. J. R. Richmond, "Organization of single motor units in feline sartorius," *J. Neurophysiol.*, vol. 72, pp. 1885-1896, 1994.
- [28] S. H. Scott, D. B. Thomson, F. J. R. Richmond, and G. E. Loeb, "Neuromuscular organization of feline anterior sartorius: II. Intramuscular length changes and complex length-tension relationships during stimulation of individual nerve branches," *J. Morphol.*, vol. 213, pp. 171-183, 1992.
- [29] D. B. Thomson, S. H. Scott, and F. J. R. Richmond, "Neuromuscular organization of feline anterior sartorius: I. Asymmetric distribution of motor units," *J. Morphol.*, vol. 21, pp. 147-162, 1991.
- [30] R. L. Lieber and J. Friden, "Muscle damage is not a function of muscle force but active muscle strain," *Amer. Physiol. Soc.*, vol. 74, pp. 520-526, 1993.
- [31] T. M. Best, C. T. Hasselman, and W. E. Garret, "Clinical aspects and basic science of muscle strain injuries," *BAM*, vol. 4, pp. 77-90, 1994.
- [32] M. A. Ariano, R. B. Armstrong, and V. R. Edgerton, "Hindlimb muscle fiber populations of five mammals," *J. Histochem. Cytochem.*, vol. 21, pp. 51-55, 1973.
- [33] L. D. Abraham and G. E. Loeb, "The distal hind-limb musculature of the cat," *Exp. Brain Res.*, vol. 58, pp. 580-593, 1985.
- [34] J. Lexell, J. Jarvis, D. Downham, and S. Salmons, "Stimulation-induced damage in rabbit fast-twitch skeletal muscles: A quantitative morphological study of the influence of pattern and frequency," *Cell Tissue Res.*, vol. 273, pp. 357-362, 1993.



Tracy Cameron (S'93-M'96) was born in Oshawa, Canada, in 1962. She received the B.Sc. degree in biochemistry from Queen's University, Kingston, Ont., Canada, in 1985; the M.S. degree in biomedical engineering from the University of Miami, Miami, FL, in 1988; and the Ph.D. degree in physiology from Queen's University in 1996.

In 1988, she worked as a Biomedical Engineer at The Miami Project to Cure Paralysis, University of Miami. There she became interested in the application of neural prosthetics to restore movement. She continued this interest during study toward the Ph.D. degree, when she was involved in the development and testing of miniature implantable stimulators. She is currently examining the application of neural prosthetics, in both the suppression of tremor and in hand opening of paretic limbs, as a Post-Doctoral Fellow at the Division of Neuroscience, University of Alberta, AB, Canada.



Tiina L. Liinamaa was born in Thunder Bay, Canada, in 1970. She received the B.Sc. degree in life sciences in 1993 and the M.Sc. degree in physiology in 1995, both from Queen's University, Kingston, Ont., Canada.

She has since worked at Queen's Bio-Medical Engineering Unit as a consultant for Advanced Bionics Corp., Sylmar, CA.

Gerald E. Loeb was born in New Jersey in 1948. He received the B.A. and M.D. degrees from the Johns Hopkins University, Baltimore, MD, in 1969 and 1972, respectively.

After a year of clinical training in surgery at the University of Arizona, Tucson, he joined the Laboratory of Neural Control at the National Institutes of Health, Bethesda, MD, as a Commissioned Officer in the Public Health Service. In his 15 years there, he worked on basic sensorimotor neurophysiology and developed many implantable transducers and electrodes for studies in unrestrained animals; more recently, this work has been extended to model-based analysis of musculoskeletal mechanics and neural control. Since 1969, he has been actively involved in clinical applications of neural prosthetics technology to restore vision (at the University of Utah, Salt Lake City), hearing (at the University of California at San Francisco), and neuromuscular control (with the A.E. Mann Foundation). He consults widely in the medical device industry and has written more than 100 journal articles, ten patients, and a textbook on electromyography. He has been at Queen's University in Kingston, Ont., Canada, since 1988, now as Director of Bio-Medical Engineering and Professor of Physiology, and serves in an advisory role as Chief Scientist of Advanced Bionics Corp., Sylmar, CA.



Frances J. R. Richmond received the B.N.Sc. degree in 1973 and the Ph.D. degree in neurophysiology in 1976.

After postdoctoral training at the National Institutes of Health in Bethesda, MD, and the Université de Montréal, Montréal, PQ, Canada, she assumed a faculty position at Queen's University, Kingston, Ont., Canada. Presently she is Professor of Physiology at Queen's University and Director of the MRC Group in Sensory-Motor Neuroscience. During this time, her interests have centered on the study of movement in diverse motor systems, with a particular focus on the neuromuscular organization, biomechanics and control of the head-movement system. This research has been complemented by a more recent program of research to understand the biological reactions and clinical usefulness of implanted electrical devices. In addition to university activities, she has served as a consultant for preclinical and clinical research activities at the Alfred E. Mann Foundation and Advanced Bionics Corp. in Sylmar, CA.